HAIL DETECTION WITH POLARIMETRIC RADAR

Edward A. Brandes*

Research Applications Program
National Center for Atmospheric Research

and

Alexander V. Ryzhkov

Cooperative Institute for Mesoscale Meteorological Studies, University of Oklahoma
and
National Severe Storms Laboratory

1. INTRODUCTION

Dual-polarization radars typically transmit horizontally and vertically polarized waves and receive polarized backscattered signals. Because illuminated hydrometeors are not spherical, their radar backscatter cross sections are not the same for the two polarizations. Hydrometeor size, shape, orientation, and thermodynamic phase can be inferred from returned signals. Polarimetric hail algorithms exploit properties of returned signals, seeking departures from the "rain-only" case. Hail location can be precisely specified. Importantly, the suite of measurements provides redundancy that can be useful for eliminating false alarms and identifying marginal events. Here the more promising proposed detection techniques are reviewed, applied to a severe hail event, and evaluated for operational use.

2. PROPOSED HAIL DETECTION ALGORITHMS

Polarimetric measurements with strong hail signatures include radar reflectivity (Z_H), differential reflectivity (Z_{DR}), linear depolarization ratio (LDR), and co-polar correlation coefficient (ρ_{HV}). [For detailed descriptions of these parameters, their usage, and typical values for different hydrometeor types see Doviak and Zrnić (1993, Chapter 8). Additional discussion of polarimetric hail signatures is given by Bringi et al. (1984, 1986), Illingworth et al. (1986), Aydin et al. (1986, 1995), Zrnić et al. (1993), and Smyth et al. (1999).] Measurements obtained with NCAR's S-Pol radar from a hail storm which produced 19 mm diameter hail in the Oklahoma panhandle on 13 June 2002 are illustrated in Fig. 1. In general, hail regions are represented by high Z_H, low Z_{DR}, relatively high LDR, and low ρ_{HV}. Large wet hail also affects the differential propagation phase (Φ_{DP}) measurement (not shown). Detection techniques examined here all depend on combinations of the Z_H, Z_{DR}, and Φ_{DP} measurements.

---

*Corresponding author address: Dr. Edward A. Brandes, National Center for Atmospheric Research, P.O. Box 3000, Boulder, C0, 80307; e-mail: brandes@ncar.ucar.edu
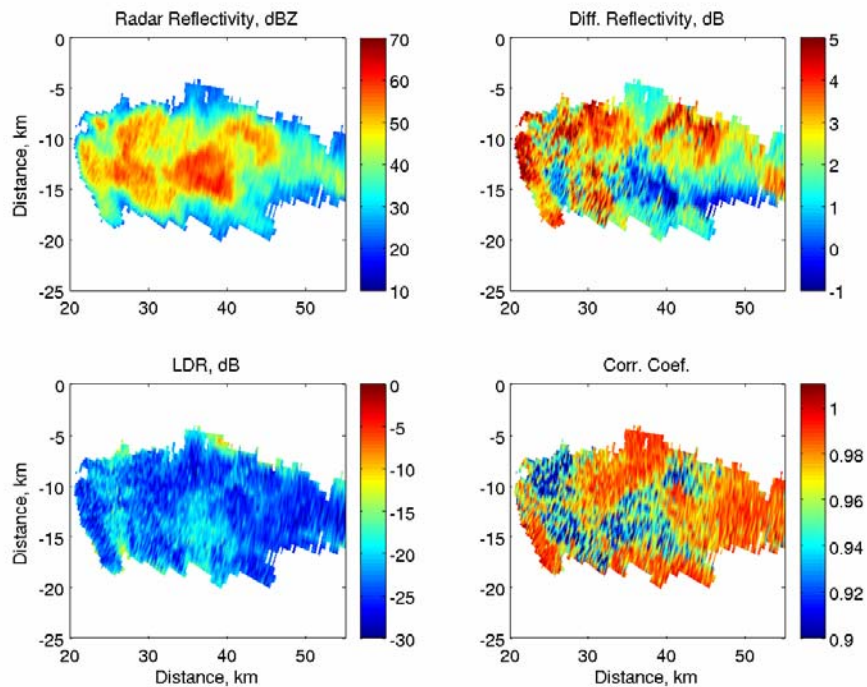
2.1 Reflectivity−Differential Reflectivity Techniques

A simple polarimetric hail-detection algorithm incorporating Z_H and Z_{DR} measurements was proposed by Leitao and Watson (1984). They determined a rain-only area in Z_H–Z_{DR} space for radar measurements obtained in the United Kingdom. A boundary, $f(Z_{DR})$, delimiting the rain distribution is

$$
\begin{aligned}
f(Z_{DR}) &= -4 Z_{DR}^2 + 19 Z_{DR} + 37.5 \text{ dB} \quad 0 < Z_{DR} < 2.5 \text{ dB} \\
&= 60 \text{ dB} \qquad\qquad 2.5 \le Z_{DR} < 4.0 \text{ dB} . \quad (1)
\end{aligned}
$$

Aydin et al. (1986) modified the Leitao and Watson method slightly, defining a hail differential reflectivity parameter (H_{DR}) given by

$$H_{DR} = Z_H - g(Z_{DR}), \qquad\qquad (2)$$

where

$$
\begin{aligned}
g(Z_{DR}) &= 27 \text{ dB} & Z_{DR} \le 0 \text{ dB} \\
&= 19*Z_{DR} + 27 \text{ dB} & 0 \le Z_{DR} \le 1.74 \text{ dB} \\
&= 60 \text{ dB} & Z_{DR} > 1.74 \text{ dB} \quad (3)
\end{aligned}
$$

The segmented line [$g(Z_{DR})$] was determined with disdrometer observations. A positive value of H_{DR} indicates hail. The likelihood of hail and hailstone size tend to increase with the magnitude of H_{DR} (Aydin et al. 1986; Brandes and Vivekanandan 1998).

Figure 2 (left panel) shows differential reflectivity measurements plotted against radar reflectivity for the 13 June storm just before hail was observed (0036 UTC). Maximum reflectivity was 56 dBZ. Associated differential reflectivity values were 4 dB—indicative of very large raindrops. The considerable scatter is attributed to DSD variations associated with strong updrafts and drop-size sorting by the storm flow.

The rain−hail boundaries (1) and (3) are overlaid in Fig. 2 (blue and red curves, respectively). Hail-contaminated measurements are expected to lie below and to the right of the curves. At 0036 UTC all Z_H-Z_{DR} measurement pairs lie in the rain-only region.

Measurements from 0041 UTC give strong hail indications (Fig. 2, right-hand panel). Data pairs to the right of the curves result from the inverse

FIG. 1: *Polarimetric radar measurements from a severe hailstorm observed in Oklahoma at 0041 UTC on 13 June 2002. The antenna elevation is 1.2°.*
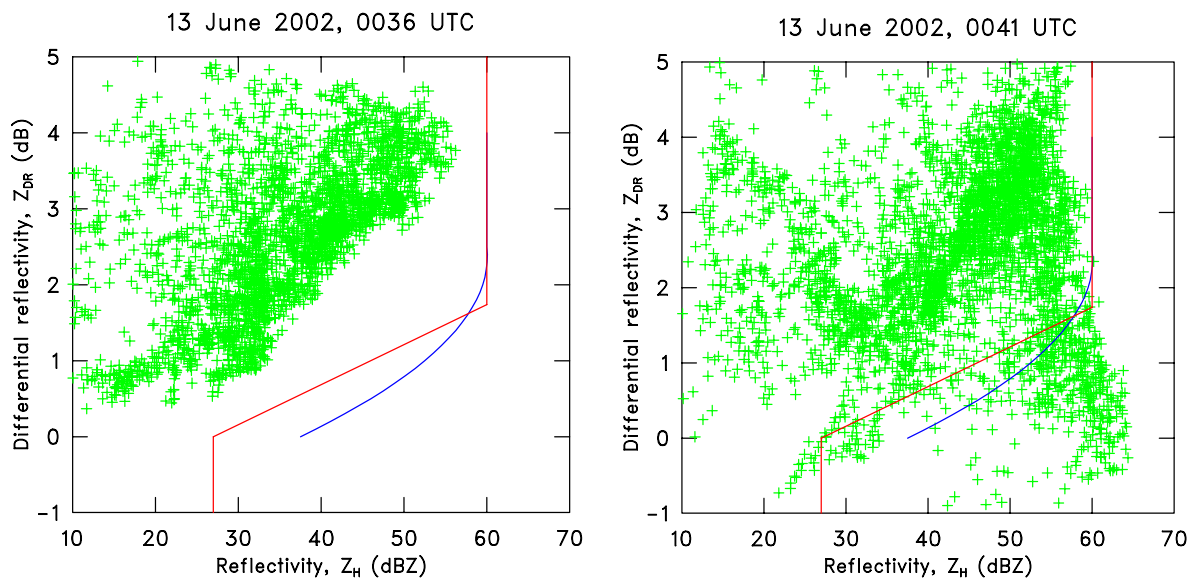

FIG. 2: *Differential reflectivity plotted against radar reflectivity for pre-hail (0036 UTC) and hail stages (0041 UTC) for the 13 June storm. The blue curve is the discriminator of Leitao and Watson [Eq. (1)], and the red curve is that of Aydin et al. (1986) [Eq. (3)]. The measurements are from 1.2° antenna elevation.*

relationship between Z_H and Z_{DR} that occurs when hail is present, whereby hail increases Z_H because of its size but reduces Z_{DR} because hail usually tumbles as it falls and has no preferred orientation. Pairs with high reflectivity and small Z_{DR} (e.g., near Z_H = 60 dBZ and Z_{DR} = 0 dB) are clearly hail affected and correctly designated by both algorithms. Measurement pairs with a Z_H of ~55 dBZ and a Z_{DR} of 2–2.5 dB are also likely contaminated by hail because they depart from the rain-only period (0036 UTC). These data points illustrate a problem with relations like (1) and (3). Data pairs along these boundaries are the limits of rain-only measurements and not typical values. They have the smallest median volume diameters for a particular reflectivity value, whereas raindrops in hailstorms are often characterized by large drops. To correctly identify these data points as hail would require a modification of (1) and (3) or a H_{DR} threshold < 0 dB. Some hail designations for Z_H ~<50 dBZ are influenced by sidelobe contamination while others arise from differential attenuation. The spatial distribution of hail designations using the algorithm of Aydin et al. (1986) is presented in Fig. 3 (H_{DR} panel). The dominance of large drops and the imposed H_{DR} threshold are believed to cause the hail region to be underestimated.

2.2 Difference Reflectivity

Golestani et al. (1989) propose to detect hail with the difference reflectivity parameter

$$Z_{DP} = 10 \log(Z_H - Z_H),$$

which is defined only for $Z_H > Z_V$. Again, the procedure for hail detection is to determine departures from the rain-only case. The radar reflectivity−difference reflectivity distribution for the rain-only stage of storm development is shown in Fig. 4a. A least-squares fit to the observations is

$$Z_{DP} = -6.831 + 1.087\, Z_H . \qquad (4)$$

Examination reveals a linear relationship with some broadening of the distribution at lower reflectivity due to a higher relative noise level in the measurements. The slope of the line and intercept are sensitive to the DSD. Smaller drop median volume diameters would associate with smaller Z_{DP} values. Application to the hail stage is presented in Fig. 4b. Radar measurements contaminated by hail lie significantly to the right of the rain-only line (4). Expectedly, the difference reflectivity shares many hail-detection attributes with differential reflectivity. Hail signatures begin at a reflectivity of approximately 50 dBZ. Because Z_{DP} is undefined for $Z_H < Z_V$, a condition most likely associated with large hail, the parameter is less desirable as a hail algorithm. Nevertheless, Z_{DP} has value as a diagnostic tool. Drawing a boundary around a region of a storm suspected to contain hail and determining a broad distribution of $Z_H - Z_{DP}$ pairs

at high reflectivity values, as in Fig. 4b, is a clear hail signature.

2.3 Fuzzy Logic Approach

Recognizing that polarimetric signatures for hail are not always unique and overlap those for other hydrometeors, fuzzy logic approaches using the suite of polarimetric measurements have been proposed (e.g., Vivekanandan et al. 1999). Membership functions are employed to determine the likelihood that a particular measurement is contaminated by hail. For example, the current membership function for reflectivity with the pure "hail" category of the real-time algorithm that operates on the S-Pol radar assigns a membership value of "0" for a reflectivity value less than 45 dBZ essentially indicating that hail is unlikely. The membership value increases linearly from 45 dBZ to 1 for a reflectivity of 50 dBZ and remains at that value for higher reflectivity values. Membership values for differential reflectivity are 1 for $Z_{DR} \leq -1$ dB and 0 for $Z_{DR} \geq 0.5$ dB. The membership function increases linearly for intermediate values. Membership function values for all radar parameters are obtained. Each parameter is then weighed for each hydrometeor classification, and the probable dominant hydrometeor type selected.

The current NCAR hydrometeor classification algorithm (HCA) makes designations for hail and rain–hail, graupel–hail, and graupel–rain mixtures. Application to the 13 June storm is shown in Fig. 3 (PID panel). A core region of hail (red, x = 37, y = −16 km) is flanked by graupel–hail and rain–hail regions. There is also an outer region of graupel–rain. While the designations seem plausible, the total areal coverage of predicted ice forms is probably overestimated. Verification of the various HCA categories will require an extended effort.

2.4 Consistency Method

This method is a variation of techniques that use radar reflectivity and specific differential propagation phase (K_{DP}, the range derivative of Φ_{DP}). Consistency among Z_H, Z_{DR}, and K_{DP} dictates that any two parameters can be used to determine the third parameter. For example, K_{DP} for rain can be estimated from Z_H and Z_{DR} (linear units) with (Vivekanandan et al. 2003)

$$K_{DP} = 3.32 \times 10^{-5} Z_H Z_{DR}^{-2.0} . \qquad (5)$$

An inconsistency arises between relations like (5) and the polarimetric measurements when hail is present (Smyth et al. 1999). A hail parameter (*HP*) can be determined as

$$HP = K_{DP,c} - K_{DP,m} , \qquad (6)$$

where $K_{DP,c}$ is the estimated value of K_{DP} computed with (5) from radial distributions of Z_H and Z_{DR}, and
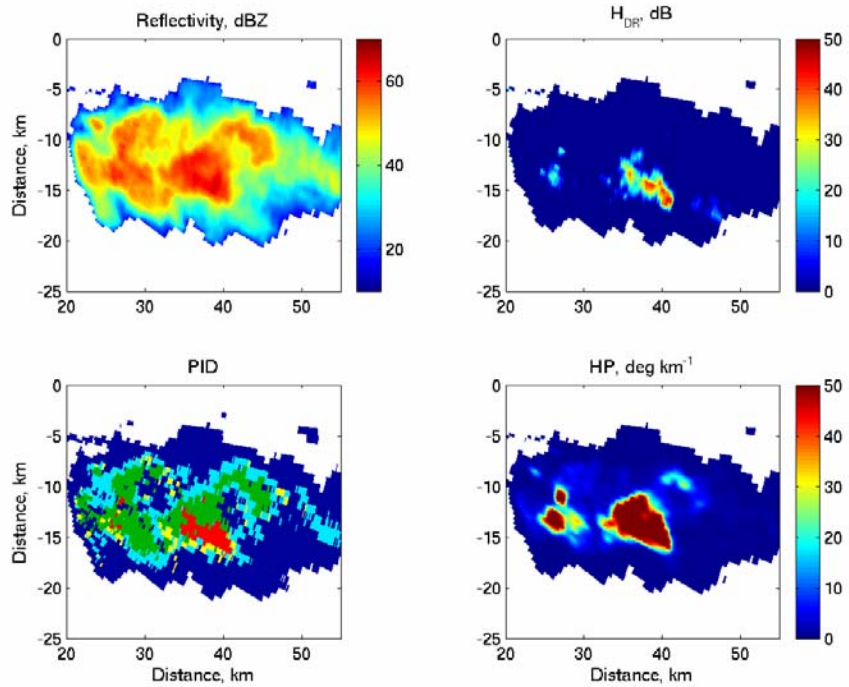
FIG. 3: *Radar reflectivity (slightly smoothed) and hail designations made with potential algorithms for the dataset in Fig. 1. PID classifications are for hail (red) and hydrometeor mixtures: graupel−hail (yellow), rain−hail (green), and graupel−rain (light blue).*
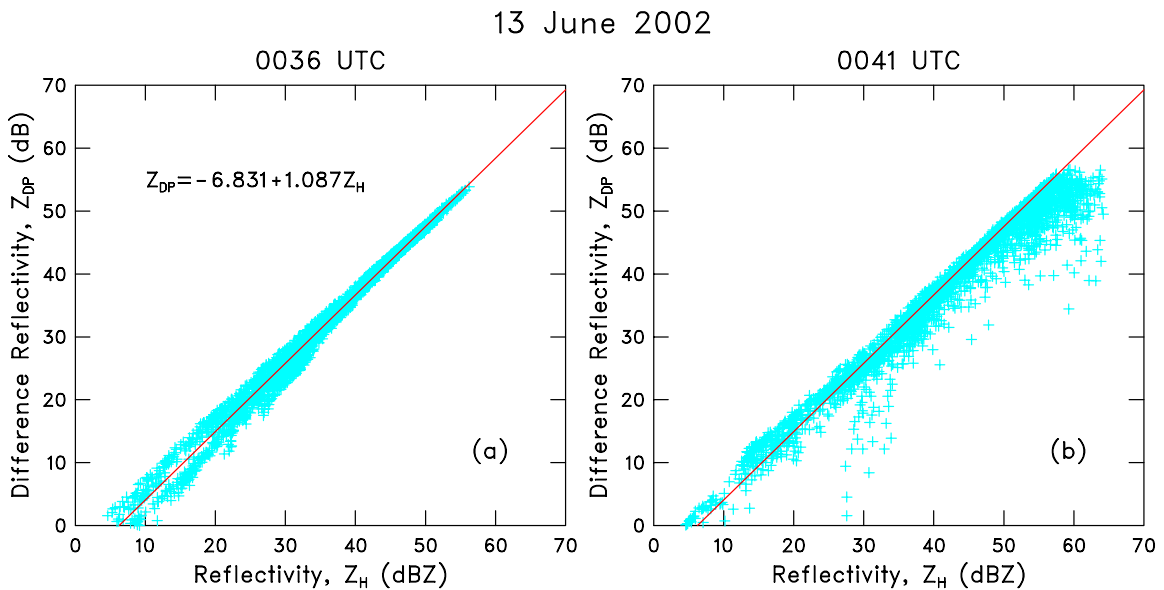

FIG. 4: *Difference reflectivity plotted against radar reflectivity for the hailstorm at (a) 0036 and (b) 0041 UTC. The red line is a least-squares fit [Eq. (4)] for the pre-hail stage (0036 UTC). The antenna elevation is 1.2^o.*

$K_{DP,m}$ is the radar-estimated specific differential phase based on Φ_{DP} measurements. Hail increases $K_{DP,c}$ relative to $K_{DP,m}$. *HP* should be close to 0° km^{-1} for rain. Significant positive departures from 0° km^{-1} would signify hail.

The *HP* parameter (Fig. 3) essentially predicts hail in the same locations determined with the fuzzy logic and H_{DR} methods. As with the other algorithms, designated hail regions are clearly separated from rain areas. However, the approach is simpler than the fuzzy logic method in that, other than the selection of Eq. (5), it has no tunable parameters and issues regarding whether the measurements represent hail or mixtures of hail and other hydrometeors are avoided. The method is relatively insensitive to DSD variations; and the magnitude of *HP*, like H_{DR}, is believed to be related to hailstone size.

3. *LDR* AND ρ_{HV}

The utility of linear depolarization ratio and correlation coefficient measurements for hail detection are not evaluated in this report. The presence of hail increases the linear depolarization ratio and decreases the correlation coefficient (e.g., Fig. 1). With the S-Pol radar *LDR* in rain averages about −27 dB. Hail can increase individual *LDR* measurements to more than −20 dB. There is considerable overlap in the rain-only and hail-contaminated distributions. Also, the measurement is susceptible to contamination by range-folded echoes, weak signals, and leakage between the horizontal and vertical channels of the radar. The correlation coefficient shows significant reductions for hail contaminated measurements. Typical values are >0.95 for rain and can be <0.90 for hail. In extreme cases, ρ_{HV} can fall below 0.75−0.85 (Ryzhkov and Zrnić 1994). Inspection of Fig. 1 suggests that hail-detection algorithms using *LDR* and ρ_{HV} in combination with Z_H should be possible, as with the $Z_H - Z_{DR}$ measurement pair, but, to date, these approaches have not been attempted.

4. VERIFICATION

An "operational" evaluation of differential reflectivity for hail detection was conducted by Lipschutz et al. (1986). The approach was based on the work of Leitao and Watson. The experimental hail-detection algorithm had a probability of detection (POD) of 0.56 compared to a radar reflectivity-based algorithm (the original NEXRAD algorithm) of 0.68. Lipschutz et al. note that many polarimetric algorithm failures were for small hail and attributed the problem to imposed parameter thresholds. [Such problems are symptomatic of DSD issues as discussed in Section 2.1.] In spite of the disappointing results, they conclude that the polarimetric technique had great potential—but needed further testing.

Nanni et al. (2000) evaluated the algorithm of Aydin et al. (1986) with measurements at 15 min intervals from a C-band radar. Observations from 330 hail pads within 75 km of the radar provided verification. Several analysis constraints were imposed to mitigate issues related to infrequent sampling and attenuation. Hail was found to be associated with H_{DR} > 13 dB rather than all positive values. [This result may indicate a Z_{DR} bias error or problems with differential attenuation.] The POD was 0.9 for radar signatures within 2 km of the hail pads. The critical success index (CSI) was 0.6, and the false alarm rate (FAR) was 0.3. Performance may have been influenced by imposed constraints which eliminated about one half of the events. The authors note that many false alarms were close to pads that recorded hail.

An examination of the fuzzy-logic approach for detecting hail has been conducted by Heinselman and Ryzhkov (2004). The method was compared to the current WSR-88D hail detection algorithm. For a sample of four cases, the polarimetric fuzzy logic algorithm outperformed the current WSR-88D reflectivity-based algorithm in terms of overall accuracy and skill. There was a small increase in the POD, a 29% decrease in the FAR, and a 26% increase in the CSI. With some algorithm tweaking, all occurrences in which observed hail was not detected were eliminated.

5. SUMMARY AND CONCLUSIONS

Polarimetric variables offer promise for improved hail detection, specifying its location, and estimating hailstone size. The biggest benefit is expected to be the designation of small hail in more marginal hailstorms. Algorithms examined here exhibit desired attributes of a detection procedure in that hail regions are readily separated from rain-only areas. Further, the magnitude of parameters, such as H_{DR} and *HP*, are related to the likelihood of hail and its size. While some techniques are more susceptible than others, all detection methods exhibit some sensitivity to DSD variations. Hence, storms with preternatural DSDs are a potential problem. However, the redundancy offered by the suite of measurements, including *LDR* and ρ_{HV}, may be important for identifying such events.

Attempts at verification generally show improved results with polarimetric measurements over algorithms based on radar reflectivity alone. Indeed, decreases in false alarm rates and increases in critical success rates of ~30% over radar reflectivity-based schemes are indicated. The verification dataset is very small. A systematic comparison among the various techniques described here and others, such as the $Z_H - K_{DP}$ procedure of Balakrishnan and Zrnić (1990), on a large dataset obtained from a variety of climatic regimes is needed.

References

Aydin, K, T. A. Seliga, and V. Balaji, 1986: Remote sensing of hail with a dual linear polarization radar. *J. Climate and Appl. Meteor.,* **25,** 1475–1484.

——, V. N. Bringi, and L. Liu, 1995: Rain-rate estimation in the presence of hail using S-band specific differential phase and other radar parameters. *J. Appl. Meteor.,* **34,** 404–410.

Balakrishnan, N., and D. S. Zrnić, 1990: Estimation of rain and hail rates in mixed-phase precipitation. *J. Atmos. Sci.,* **47,** 565–583.

Brandes, E. A., and J. Vivekanandan, 1998: An exploratory study in hail detection with polarimetric radar. *Preprints,* 4th International Conference on Interactive Information and Processing Systems for Meteorology, Oceanography, and Hydrology, Phoenix, Arizona, Amer. Meteor. Soc., 287–290.

Bringi, V. N., T. A. Seliga, and K. Aydin, 1984: Hail detection with a differential reflectivity radar. *Science,* **225,** 1145–1147.

——, J. Vivekanandan, and J. D. Tuttle, 1986: Multiparameter radar measurements in Colorado convective storms. Part II: Hail detection studies. *J. Atmos. Sci.,* **43,** 2564–2577.

Doviak, R., and D. Zrnić, 1993: *Doppler Radar and Weather Observations*, Academic Press, 562 pp.

Heinselman, P., and A. V. Ryzhkov, 2004: Hail detection during the Joint Polarization Experiment. *Preprints,* 22nd Conf. on Severe Local Storms, Hyannis, Massachusetts, Amer. Meteor. Soc.

Illingworth, A. J., J. W. F. Goddard, and S. M. Cherry, 1986: Detection of hail by dual-polarization radar. *Nature,* **320,** 431–433.

Leitao, M. J., and P. A. Watson, 1984: Application of dual linearly polarized radar data to prediction of microwave path attenuation at 10–30 GHz. *Radio Sci.,* **19,** 209–221.

Lipschutz, R. C., J. F. Pratte, and J. R. Smart, 1986: An operational Z_{DR}-based precipitation type/intensity product. *Preprints,* 23rd Conf. on Radar Meteorology, Snowmass, Colorado, Amer. Meteor. Soc., JP-91–JP-94.

Nanni, S., P. Mezzasalma, and P. P. Alberoni, 2000: Detection of hail by polarimetric radar data and hailpads: Results from four storms. *Meteorol. Appl.,* **7,** 121–128.

Ryzhkov, A. V., and D. S. Zrnić, 1994: Precipitation observed in Oklahoma mesoscale systems with polarimetric radar. *J. Appl. Meteor.,* **33,** 455–464.

Smyth, T. J., T. M. Blackman, and A. J. Illingworth, 1999: Observations of oblate hail using dual polarization radar and implications for hail-detection schemes. *Quart. J. Roy. Meteor. Soc.,* **125,** 993–1016.

Vivekanandan, J., G. Zhang, S. M. Ellis, D. Rajopadhyaya, and S. K. Avery, 2003: Radar reflectivity calibration using differential propagation phase measurement. *Radio Sci.,* **38,** doi:10.1029/2002RS002676.

——, D. S. Zrnić, S. M. Ellis, R. Oye, A. V. Ryzhkov, and J. Straka, 1999: Cloud microphysics retrieval using S-band dual-polarization measurements. *Bull. Amer. Meteor. Soc.,* **80,** 381–388.

Zrnić, D. S., V. N. Bringi, N. Balakrishnan, K. Aydin, V. Chandrasekar, and J. Hubbert, 1993: Polarimetric measurements in a severe hailstorm. *Mon. Wea. Rev.,* **121,** 2223–2238.